Nuclear Inst. and Methods in Physics Research B 448 (2019) 52–56

Contents lists available at ScienceDirect

Nuclear Inst. and Methods in Physics Research B

journal homepage: www.elsevier.com/locate/nimb

Light particle spectroscopy using CR-39 detectors: An experimental and simulation study

H. Elazhar[a,*], A.C. Chami[b], M. Abdesselam[b], N. Arbor[a], D. Muller[c], A. Nasreddine[a], M. Roumie[d], Z. El Bitar[a,e], A. Nourreddine[a]

[a] Institut Pluridisciplinaire Hubert Curien (IPHC), Universitéde Strasbourg, 23 rue du Loess, 67037 Strasbourg Cedex, France
[b] Faculté de Physique, Universitédes sciences et de la Technologie d'Alger, BP 32 El Alia, 16111 Bab Ezzouar Algeria
[c] Laboratoire ICube, CNRS-Université de Strasbourg, 23 rue du loess, 67037 Strasbourg, France
[d] Ion Beam Analysis Laboratory, Lebanese Atomic Energy Commission, National Research for Scientific Research, P.O. Box 11-8281, Beirut, Lebanon
[e] Laboratory of Physics and Modeling, EDST, Lebanese University, 1300 Tripoli, Lebanon

ARTICLE INFO

Keywords:
Solid state nuclear track detectors
CR-39
Alpha tracks
Proton tracks
Chemical etching

ABSTRACT

CR-39 detectors have been irradiated with both ^{241}Am alpha particles and protons in the energy range of 1.0–5.5 MeV and 0.8–2.8 MeV, respectively. The proton irradiation has been achieved through two different techniques: Rutherford Backscattering (RB) and Nuclear Reaction (NR). The detectors were chemically etched in a hot KOH solution for periods ranging from 0.5 h to 3 h for alpha particles and 2.5 to 5.5 h for protons. The track diameter variation as a function of particles energies and etching time has been studied. A new predictive model based on experimental track parameters has been developed for the studied particles and for variable bulk track etching velocities. This predictive model is based on a single parameter β determined by fitting our experimental data.

1. Introduction

Solid state nuclear track detectors (SSNTDs) are used in many applications as detectors of protons or alphas which include neutron detection and dosimetry [1], cosmic-ray physics [2], and different medical applications such as radio/hadron therapy [3]. The most popular kind of SSNTD used for proton and alpha detection is the polyallyldiglycol carbonate (PADC) film, commercially known as CR-39. When charged particles pass through the material, they induce damaged regions along the incident particle trajectory, which are referred to as latent tracks. Typically having diameters of about 5–10 nm around the incident particle trajectories, the latent tracks are chemically more active than the surrounding undamaged area and thus can be enlarged through chemical or electrochemical etching with aqueous solutions of aggressive chemicals (NaOH or KOH). These kinds of detectors can be employed to register the tracks caused by various types of heavy charged particles. Thanks to the track density (number of tracks per unit area) revealed on the detector, the incident particle fluence can be determined. However, in some cases like the neutron radiation protection field, both the particle fluence and particles energy are required. In such field, one of the challenging tasks is to have the neutron energy information to evaluate equivalent doses from neutrons, which are dependent upon the neutron energies. The basic tool for studying or counting the tracks in SSNTDs is the optical microscope [4,5]. The track analysis can be achieved through automatic or semi-automatic counting and image analysis [6]. Several works have been described in books and review papers in order to study the process and condition for etching on the track parameters [4,7], and several softwares have been developed for the simulation of the development of proton tracks in PADC films [8,9]. However, while in most codes simulating the track profile, the bulk etch rates (V_B) are assumed to have constant values (i.e time independent), no model has been developed for track parameter prediction when variable V_B is involved. Indeed, in the literature, it has been reported that V_B is variable and can be considered as constant only after a few hours of etching [10,11]. This has been explained to be due to the hardness of the surface layer of the detector, which was in contact with the casting glass plate during the manufacturing procedure [10]. Moreover, V_B is also known as being influenced by many factors, such as the intrinsic characteristics of the plastic material due to its chemical composition, preparation method and the etching conditions in terms of temperature, concentration and type of etchant, etching duration, stirring etc. In most of the studies, V_B is always considered as being a constant parameter between successive etchings, while from one etching to another, as just mentioned, it can vary if the temperature and

* Corresponding author.
E-mail address: halima.elazhar@iphc.cnrs.fr (H. Elazhar).

https://doi.org/10.1016/j.nimb.2019.04.012
Received 14 December 2018; Received in revised form 27 March 2019; Accepted 4 April 2019
0168-583X/ © 2019 Published by Elsevier B.V.

solution concentration are difficult to keep constant during the etching, and if stirring of the solution is involved [5].

The aim of our work was thus to study the variation of proton and alpha track parameters for variable V_B. The experimental results obtained through the processing of CR-39 detectors irradiated, with an ^{241}Am alpha source and with proton beams through nuclear reactions and Rutherford backscattering (RB) techniques, have been compared to a track diameter predictive model for variable V_B. Thanks to this model, a charged particle spectroscopy and thus indirectly a neutron spectroscopy can be feasible, even for non-optimal etching conditions.

2. Irradiations

CR-39 from Technol Chyoda (Japan) with an area of 19 × 8.5 mm^2 and 0.8 mm thickness have been used for this study. Before irradiating the CR-39 detectors by protons and alpha particles, charged particle spectroscopy (He,H) were performed using a data acquisition system consisting of a charged-particle Si detector (Ultra + series), a charge sensitive preamplifier, a spectroscopy amplifier, an analog-digital converter and a computer equipped with an acquisition card. The experiments permit the measurement of the energy and fluence of the irradiation.

Irradiations with different light charged particles have been done. For the alpha particles, a thin ^{241}Am source has been used. The energy spectrum of the emitted α-particles contains mainly two energy groups of 5.486 MeV and 5.443 MeV with relative intensities of 85.2% and 12.8% respectively. Up to 8 stacked self-supporting thin PET foils 3.6 µm thick have been interposed between the source and the detector [12] to degrade the energy of the transmitted beam from 5.486 MeV with no PET film to 1.067 MeV with 8 PET films.

The proton irradiations were performed at the Lebanese Atomic Energy Commission facility (Beyrouth, Lebanon) with backscattered particles from a thin Ni self-supported target. Backscattered [13] energies range from 0.867 to 2.775 MeV. They were measured by positioning the Si detector (Ultra +) and the CR-39 detectors at 145° at each side of the incident beam. The backscattered particles were energetically analyzed by the Si detector and the fluence irradiation was given by the Ni peak area.

Proton irradiations on CR-39 were also performed with proton groups arising from nuclear reactions (NR) [13]. In this experiment, 0.9 MeV deuterons delivered by the 4 MV Van de Graaff accelerator of the ICube laboratory in Strasbourg were used. A very thin film of carbon (5×10^{16} atoms/cm^2) was evaporated on a SiO_2 target of 1×2.10^{18} atoms/cm^2. This target was mounted at the center of the reaction chamber perpendicular to the incident deuteron beam to produce a secondary proton beam. The proton groups from the reactions $^{12}C(d,p_0)^{13}C$, $^{16}O(d,p_0)^{17}O$ and $^{16}O(d,p_1)^{17}O^*$ were collected by the silicon detector with respective CR-39 irradiation energies: E_p = 2.753 MeV, 2.130 MeV and 1.266 MeV. The Si detector and a CR-39 detector were positioned at 150° at each side of the incident beam. A Mylar foil of 12 µm thickness was set in front of each detector to eliminate the α-particles arising from the $^{16}O(d,\alpha)^{14}N$ reaction and the backscattered deuterons.

3. Chemical etching and microscopic reading

Latent tracks produced by protons and alpha particles have been revealed by chemical etching in a 30% potassium hydroxide (KOH) solution at a temperature of 90 ± 3 °C. During the etching process, the etchant was continuously stirred to assure its homogeneity, according to Rana and Qureshi [14]. The detectors have been etched at different etching times ranging from 0.5 h to 3 h for alpha particles and from 2.5 h to 5 h for protons, with 0.5 h steps. After every etching, the detectors were immersed in dilute HCl for 15 min, rinsed in distilled water and dried in order to definitively stop the etching process by removing any KOH that may still be present on the detectors. The mass of each detector was determined before and after each etching by using a balance with an accuracy of ±10 µg in order to access the bulk etch rate values method such as [5]:

$$V_B = \frac{\Delta m}{2A\rho t} \quad (1)$$

where Δm is the mass difference, A the etched surface area, ρ the density of the detector and t is the etching time.

The V_B values are reported in Tables 1 and 2 respectively for the alpha and proton exposures. Alpha and protons track diameter measurements were then performed at the detector surface using an automatic analyzing system. It consists of a CCD camera mounted on an optical microscope (10× magnification) with a motorized XYZ stage piloted by a PC. Images of 85 optical fields forming a scanned area of about 46 mm^2 of each detector were acquired and saved. All track images were processed under the same conditions and analyzed.

Table 1
Alpha particles on CR-39 (V_B values).

Etching time [h]	0.5	1	1.5	2	2.5	3
V_B [µm.h^{-1}]	9.3	6.0	9.7	13.3	12.4	15.3

Table 2
Protons on CR-39 (V_B values).

Etching time [h]	2.5	3	3.5	4	4.5	5	5.5
V_B [µm.h^{-1}]	8.0	11.9	18.7	25.0	22.4	26.9	27.7

4. Model description

4.1. β parameter effect

The aim of this model is to calculate the diameter D(E,t) of the tracks induced by a light ion of energy E in the CR-39 as a function of the etching time t for various bulk etching rates. It can also calculate the etch profile of a swift charged particle in those conditions. The variation of the track etch rate along the particle trajectory has been studied [5,15,16]. The simplest case of track development treated here refers to that when the incident particle enters a detector under normal incidence with respect to the detector surface (Fig. 1).

t_0 is the time the chemical etching reaches the point P of abscissa $X_T(t_0)$ and $V_T(t_0)$ is the corresponding track etching rate. The developed model is based on the dependence of V_T on the bulk etching rate (V_B) and the restricted stopping power $S_\Delta(X_T)$ [17] through a parameter β according to the following formula:

$$V_T = V_B(1 + \beta S_\Delta(X_T)) \quad (2)$$

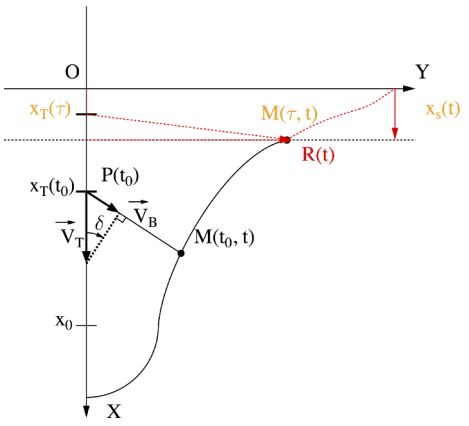


Fig. 1. Geometry of the track development for a normal incidence.

At a time $t > t_0$, the chemical etching will propagate in the CR-39 detector with a bulk etching velocity V_B along a direction defined by an angle δ (Fig. 1) such as:

$$\sin\delta(t_0) = V_B/V_T(t_0) \quad (3)$$

Replacing V_T by its value with respect to V_B in Eq. (3) we get:

$$\sin\delta(t_0) = [1 + \beta S_\Delta(X_T)]^{-1} \quad (4)$$

The coordinates of the point M (Fig. 1) reached by the chemical etching after a time t are:

$$X_M = X_T(t_0) + V_B(t - t_0)\sin\delta(t_0) \quad (5)$$

$$Y_M = V_B(t - t_0)\cos\delta(t_0) \quad (6)$$

The diameter D(E,t) is given by $2\times Y_M$.

The parameter β has been determined by minimizing the deviation between the estimated diameter D(E,t), and the measured values as:

$$Q(\beta) = \sqrt{\sum_{i=1}^{n} |Y^2_{cal}(t_i, E) - Y^2_{mes}(t_i, E)|} \quad (7)$$

with t_i duration of etching i, E particle energy, Y_{cal} the estimated radius and Y_{mes} the experimentally measured radius. The selection of the β value is such that $Q(\beta)$ is minimal.

The calibration procedure consists in irradiating the detectors with protons or alpha particles having a known energy, than to proceeding to a chemical etching interrupted periodically in order to acquire images of the detector and to measure the depth of the etched zone and the track diameters. Hence, a Look-Up Table (LUT) will be created enabling to estimate the energy and the type of the particle given the etching time, the depth of the etched zone and the track diameter. For alpha particles, the β parameter has shown no dependence upon the particle energy and the etching conditions: it has been estimated to have a value of 0.025 cm/MeV. However for protons, it appeared to be strongly dependent upon the energy. Fig. 2 represents the variation of the β parameter as a function of the proton energy which follows an exponential law as:

$$\beta(E) = a \times \exp^{-E/b} \quad (8)$$

with a = 0.06885 cm/MeV and b = 0.577 MeV.

4.2. Track profile prediction

The model is also used for track profile prediction for various projectiles, incident energy, etching time and bulk rate etching. The predicted etched track profiles for a 5.486 MeV alpha particles are reported on Fig. 3 as a function of etching time. As per the model prediction, depending on the etching time, the track profile goes from a conical track, to a partially conical and partially spherical track. For long etching time, where the bulk thickness is above the particle range in the detector material, the predicted profile shows a fully spherical shape of the track. These predictions are in good agreement both with the model described by Nikezic and Yu (Fig. 2 of [5]) and with Fromm et al. [18] observation for Lithium ion.

An experimental validation of the predicted profile will be carried out as the next step of our work.

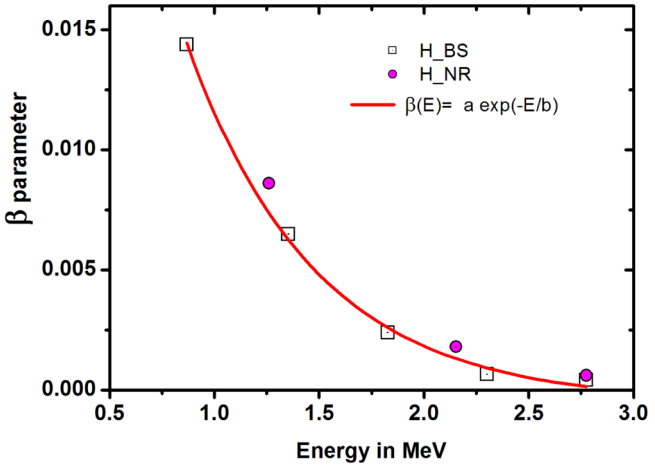


Fig. 2. Proton β parameter variation as a function of incident proton energies.

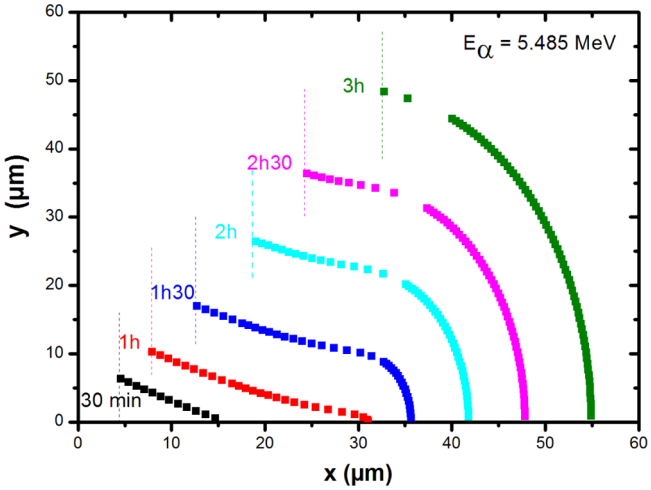


Fig. 3. Predicted alpha track profile as a function of etching time.

5. Results and discussion

5.1. Alpha particles

The variation of the track diameter as a function of alpha particle energy at selected values of the etching time ranging from 0.5 h to 3 h is shown in Fig. 4. These results show weak energy dependences for etching time lower than 2 h.

As expected, for an etching time greater than 2 h, the track diameters increase with incident energy. This dependence corroborates our assumption that $V_T = f(S_\Delta)$. When the etching time increases, a maximum diameter is observed at incident energy around 3 MeV for t = 2 h, and this maximum tends to shift slightly to higher energies, when we extend the etching time. It can be observed around 4.6 MeV

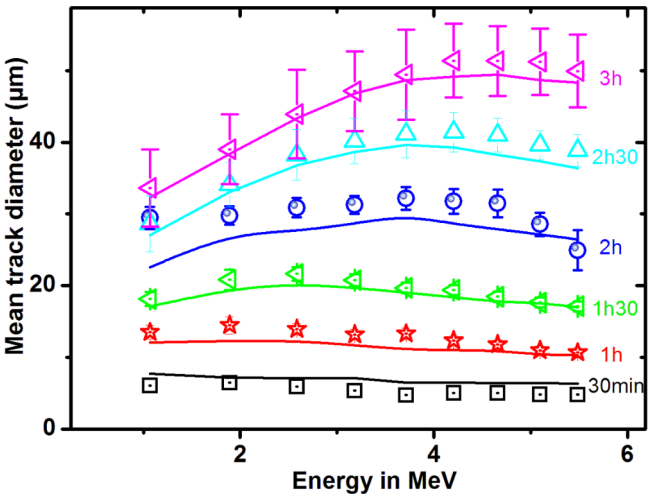


Fig. 4. Track diameters as a function of alpha particle energy and etching time. The symbols represent the experimental values and the continuous line the model predictions. The parameter β = 0.025 cm/MeV is taken as constant.

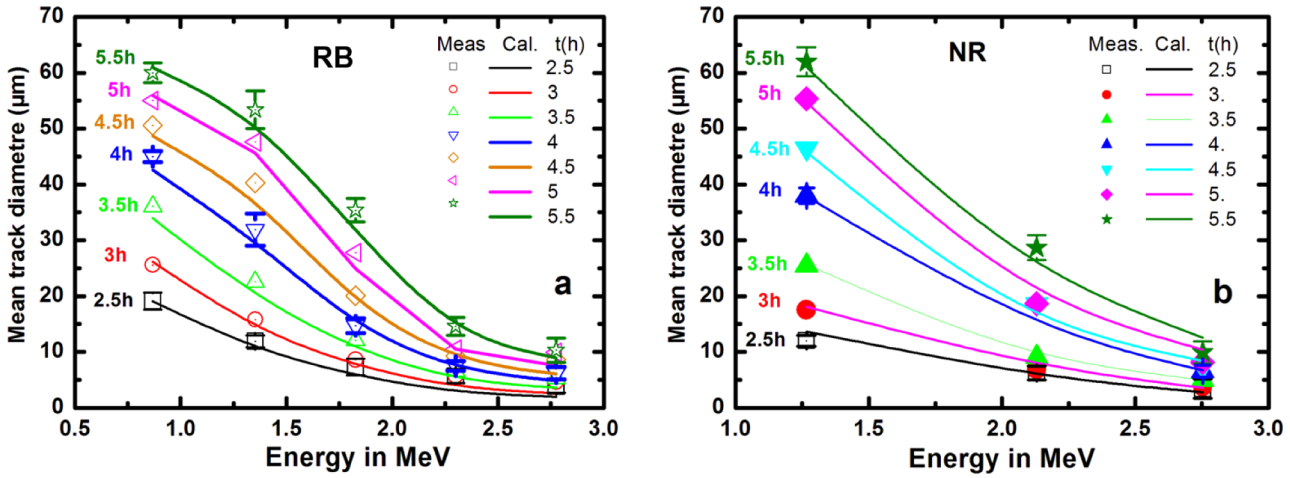


Fig. 5. a – Track diameters as a function of proton energy and etching time. The empty symbols represent the experimental values for Rutherford Backscattering (RB) proton irradiations. The continuous line represents the model predictions; b – Track diameters as a function of proton energy and etching time. The filled symbols represent the experimental values for the Nuclear Reaction (NR) on ^{12}C and ^{16}O. The continuous line is the model predictions. The parameter $\beta = 0.025$ cm/MeV is taken as constant.

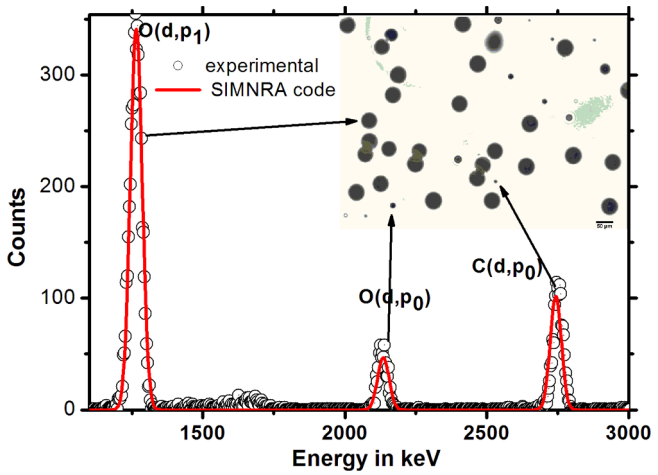


Fig. 6. Energy spectra of protons from NR and typical corresponding track images obtained after 4h30 of etching. The empty curves and solid line represent respectively measured and NRA spectra simulations using the SIMNRA code [19].

for t = 3 h. This shift in the maximum track diameter can be related to the total amount of the particle energy loss, i.e, around the range.

On the same figure, we have also represented in continuous lines the variation of the tracks diameter as a function of the energy and etching time predicted from the proposed model. The model is in reasonable agreement with the experimental results within the margin of the experimental errors.

5.2. Protons

The variation of the track diameter as a function of proton incident energies at selected values of the etching time ranging from 2.5 h to 5.5 h is shown in Fig. 5 for RB and NR irradiations. Both types of measurements are coherent. Within the studied proton energy range, it appears that the track diameter decreases monotonously with the proton energy. As can be seen in Fig. 5 both for RB and NR, the energy dependency is more important for high etching times. This decrease reflects the stopping power energy dependence.

Comparison between the NR and RB protons track diameters are in good agreement with the used model. Similarly to the alpha particles, the model reproduces well the same track diameter evolution as the experiment, within the experimental errors.

On the one hand, as shown in Fig. 6, a clear discrimination is established between the different energy groups of protons. On the other hand, the number of tracks of a given energy is proportional to the corresponding peak area.

6. Conclusion

CR-39 detectors have been irradiated with both ^{241}Am alpha particles and protons in the energy range of 1.0–5.5 MeV and 0.8–2.8 MeV, respectively. The proton irradiations were made by two different techniques: Rutherford Backscattering and Nuclear Reactions.

The development of a track parameter predictive model could be made for variable V_B of alpha particles and protons. This model that relies on a beta (β) parameter found to be constant for alpha particles and obeying an exponential law for protons has shown predictions in reasonable agreement with various experimental results for different alpha and proton energies and etching conditions. The predicted track profile showed a good agreement with the models reported in the literature. Finally the fact that the parameter β is energy dependant indicates that the restricted stopping power does not alone define locally the value of the track etching rate.

The next steps of this work would be first to validate the predicted track profile before testing it for non-variable V_B on a wider energy range and for various projectiles. This work would then be followed by the validation of this model for charged particles with variable incident angles.

Acknowledgements

This work was partially funded by the “Projet International de Coopération Scientifique” (PICS 6509) between the French CNRS, the Lebanese CNRS, the Lebanese University and the Saint Joseph University of Beyrouth.

References

[1] M. Caresana, M. Ferrarini, A. Parravicini, A. Sashala Naik, Dose measurements with CR-39 detectors at the CERF reference facility at CERN, Radiat. Meas. 71 (2014) 502.
[2] L. Tommasino, Detectors/dosemeters of galactic and solar cosmic rays, Radiat. Prot. Dosim. 109 (2004) 365.
[3] B. Smilgys, S. Guedes, M. Morales, F. Alvarez, J.C. Hadler, P.R.P. Coelho,

P.T.D. Siquiera, I. Alencar, C.J. Soares, E.A.C. Curvo, Boron thin films and CR-39 detectors in BNCT: a method to measure the 10B(n,α)7Li reaction rate, Radiat. Meas. 50 (2013) 181.
[4] S.A. Durrani, R.K. Bull, Solid State Nuclear Track Detection: Principles, Methods and Applications, Pergamon, 1987.
[5] D. Nikezic, K.N. Yu, Formation and growth of tracks in nuclear track materials, Mater. Sci. Eng. R Rep. 46 (2004) 51.
[6] D. Nikezic, K.N. Yu, Theoretical feasibility study on neutron spectrometry with the polyallyldiglycol carbonate (PADC) solid-state nuclear track detector, Nucl. Instr. Methods Phys. Res. Sect. A 771 (2015) 134.
[7] C. Hepburn, A.H. Windle, Solid state nuclear track detectors, J. Mater. Sci. 15 (1980) 279.
[8] P. Sabyasachi, S.P. Tripathy, P.K. Sarkar, Analysis of 3-dimentional track parameters from 2-dimensional images of etched tracks in solid polymeric track detectors, Nucl. Instr. Methods Phys. Res. Sect. A 690 (2012) 58.
[9] D. Nikezic, M. Ivanovic, K.N. Yu, A computer program TRACK_P for studying proton tracks in PADC detectors, SoftwareX 5 (2015) 74.
[10] M. Yamamoto, N. Yasuda, M. Kurano, T. Kanai, A. Furukawa, N. Ishigure, K. Ogura, Atomic force microscopic analyses of heavy ion tracks in CR-39, Nucl. Instr. Methods Phys. Res. Sect. B 152 (1999) 349.
[11] A. Malinowska, A. Szydlowski, M. Jaskòla, A. Korman, B. Sartowska, T. Kuehn, M. Kuk, Investigations of protons passing through the CR-39/PM-355 type of solid state nuclear track detectors, Rev. Sci. Instrum. 84 (2013) 073511 .
[12] S. Kumar, P.K. Diwan, Shyam Kumar, Energy loss straggling for α-particles in varying thicknesses of Al, Ti and Ni metallic foils, Radiat Phys. Chem. 106 (2015) 21.
[13] J.R. Tesmer, M.A. Nastasi, Handbook of modern ion beam materials analysis, Mater. Res. Soc. (1995).
[14] A.R. Mukhtar, I.E. Qureshi, Studies of CR-39 etch rates, Nucl. Instr. Methods Phys. Res. Sect. B 198 (2002) 129.
[15] D. Hermsdorf, Measurement and comparative evaluation of the sensitivity V for protons and hydrogen isotopes registration in PADC detectors of type CR-39, Radiat. Meas. 44 (2009) 806.
[16] D. Hermsdorf, M. Hunger, Determination of track etch rates from wall profiles of particle tracks etched in direct and reversed direction in PADC CR-39 SSNTDs, Radiat. Meas. 44 (2009) 766.
[17] B. Dörschel, J. Henninger, Program StopPow – a useful tool for computation of energy loss and range of light ions in SSNTDs, Nucl. Instr. Methods Phys. Res. Sect. B 171 (2000) 423.
[18] M. Fromm, F. Vaginay, G. Meesen, A. Chambaudet, A. Poffijn, Watching at the correlation between the specific track-etch rate and the primary physical parameters of the swift ion interaction with the CR-39, Radiat. Meas. Pergamon, 2003, p. 93 vol. 36.
[19] Matej Mayer, SIMNRA Computer simulation of RBS, ERDA and NRA by Matej Mayer, 2015. URL:https://home.mpcdf.mpg.de/mam/.